http://dx.doi.org/10.5012/bkcs.2013.34.4.1232

Structural Analysis of Cu Binding Site in $[Cu(I)\cdot d(CpG)\cdot d(CpG)-2H]^{-1}$ Complex

Yu-Jin Im, Sang-Mi Jung, Ye-Song Kang, and Ho-Tae Kim*

Department of Applied Chemistry, Kumoh National Institute of Technology, Gumi 730-701, Korea
**E-mail: hotaekim@kumoh.ac.kr*
Received March 27, 2013, Accepted March 28, 2013

The Cu cation binding sites of $[Cu(I)\cdot d(CpG)\cdot d(CpG) - 2H]^{-1}$ complex have been investigated to explain the [Cu·DNA] biological activity caused by the Cu association to DNA. The structure of $[Cu(I)\cdot d(CpG)\cdot d(CpG) - 2H]^{-1}$ complex was investigated by electrospray ionization mass spectrometry (ESI-MS). The fragmentation patterns of $[Cu(I)\cdot d(CpG)\cdot d(CpG) - 2H]^{-1}$ complex were analyzed by MS/MS spectra. In the MS/MS spectra of $[Cu(I)\cdot d(CpG)\cdot d(CpG) - 2H]^{-1}$ complex, three fragment ions were observed with the loss of d(CpG), {d(CpG) + Cyt}, and {d(CpG) + Cyt + dR}. The Cu cation binds to d(CpG) mainly by substituting the H^+ of phosphate group. Simultaneously, the Cu cation prefers to bind to a guanine base rather than a cytosine base. Five possible geometries were considered in the attempt to optimize the $[Cu(I)\cdot d(CpG)\cdot d(CpG) - 2H]^{-1}$ complex structure. The *ab initio* calculations were performed at B3LYP/6-31G(d) level.

Key Words : d(CpG), d(CpG)·d(CpG) dinucleotide duplex, $[Cu(I)\cdot d(CpG)\cdot d(CpG) - 2H]^{-1}$ complex, Mass spectrometry (MS), MS/MS

Introduction

The influence of metal ions on the DNA characteristics has been investigated over the past several decades.[1-5] Metal ions are known to have specific effects on the structure and stability of DNA molecule. Metal ion interactions with DNA are critical for many biological processes such as respiration, gene regulation, and photosynthesis.[6-8] Metal ions can both stabilize and destabilize DNA.[5,9,10] However, several divalent metal ions destabilize DNA and decrease the mean temperature of transition (T_m) value of DNA.[5] Specifically, there is a substantial effect of the Cu cation on T_m and on the conformation transformation (B-DNA→Z-DNA) of DNA.[5,11,12] Interaction of Cu cation with DNA as a part of [metal·DNA] complex have also been studied extensively using IR,[13,14] X-ray,[12,15] along with other techniques.[16,17] Cu cation prefers to interact with the backbone phosphate negative groups through nonspecific electrostatic attraction, which stabilizes the DNA helix structure.[14,18] However, several experimental results showed that DNA base sites had also been regarded as preferred binding sites in the formation of the [Cu·DNA] complex.[5,14,18-20]

The effect of the Cu cation on the structure of DNA was investigated to analyze the structures of dinucleotide duplex,[20] mononucleotide[21] and nucleoside,[22,23] complexed with Cu cation. Two different cross-section conformers, globular geometry and Watson-Crick geometry, were suggested in the $[Cu\cdot d(CpG)\cdot d(CpG)]^{+1}$ arrival time distribution (ATD) observations. It was explained that the soft acids and borderline acids with d^9 (Cu^{2+}) and d^{10} (Zn^{2+}) shells stabilize both globular and Watson-Crick geometries while other alkali and alkali-earth metal cations yield a globular geometry in the $[Metal\cdot d(CpG)\cdot d(CpG)]^{+1}$ complex. In their ATD experimental analysis, however, the [phosphate-Cu-N7(guanine)] binding geometry was not considered, which was observed in the high Cu cation concentration IR experiments.[14,18] The [phosphate-H-N7(guanine)] binding geometry was also suggested in the $[H+d(CpG)]^{+1}$ complex, as observed from the ESI-MS collision-induced dissociation (CID) fragment pattern analysis.[24]

At high Cu cation concentrations, the Cu cation has been shown to be associated with DNA base sites.[19] Two forms (Watson-Crick and interstrand forms) have been proposed as the probable Cu cation binding complex structures in the spectroscopic experimental results of the [Cu·DNA] complex.[12,19,25] Baker *et al.* also suggested two more structures, globular and Watson-Crick base pair structures, in their $[Cu(I)\cdot d(CpG)\cdot d(CpG)]^{+1}$ complex cross-section analysis.[20] Several theoretical research groups have proposed the N7 position of guanine as a binding site of Cu cation (or H^+) in the cytosine-guanine complex.[26-30] The N7 position of guanine, which is an easily accessible site in the major groove of the DNA double helix structure, is the preferred metal binding site.[25,31] Many other sites, such as N3 of cytosine and N1 of adenine, were blocked by hydrogen bonding in a [Cu·DNA] complex.

In the present study, we have focused our attention on the formation and fragmentation pattern analysis of gas-phase $[Cu(I)\cdot d(CpG)\cdot d(CpG) - 2H]^{-1}$ complex using ESI-MS and tandem mass spectrometry (MS/MS) methods. Complexes of $[Cu(I)\cdot d(CpG)\cdot d(CpG) - 2H]^{-1}$ were formed in solution and electrosprayed onto the quadrupole ion guide with N_2 gas. ESI-MS was supposed to produce an intact gas-phase $[Cu(I)\cdot d(CpG)\cdot d(CpG) - 2H]^{-1}$ complex ions from molecules in solution.[15-17] The interaction sites between the Cu and $[d(CpG)\cdot d(CpG) - 2H]^{-1}$ complex were investigated in aqueous solution. *Ab initio* calculation was performed to explain the $[Cu(I)\cdot d(CpG)\cdot d(CpG) - 2H]^{-1}$ complex ion geometries

and the stabilization energies.

Experimental

The gas-phase [Cu(I)·d(CpG)·d(CpG) – 2H]$^{-1}$ complex ion was formed using the ESI-MS method. The experimental MS and MS/MS data of the fragmentation pattern analysis were obtained using a Thermo Finnigan LTQ mass spectrometer (Thermo Electron Corporation, San Jose, CA, USA).

LTQ Mass Spectrometer Conditions. All spectra were acquired in the negative ion mode over a range of *m/z* 250-2000 by averaging 60 scans. The heated capillary temperature was set at 200 °C in order to facilitate efficient complex formation. The electrospray needle voltage was set at 3.1-3.3 kV. Nitrogen was used as the sheath gas (flow, 20 units) and auxiliary gas (flow, 1 unit) in the ESI region. The samples were introduced into the electrospray interface by a direct infusion method using a microsyringe pump (SGE, Australia) at a flow rate of 5 μL/min. The MS/MS spectra were acquired with experimental conditions that consisted of an isolation width of 1 *m/z*, an activation time of 10 ms, and q_z of 0.25. In the MS/MS mode, the parent ion molecules were manually selected one by one, and each was subjected to the CID process.

Reagents. d(CpG) (CG 100%, Sigma-Aldrich Korea), $CuCl_2$ (99.999%, Sigma-Aldrich Korea), and H_2O (HPLC grade, Merck & Co.) were used in these experiments. d(CpG) was dissolved in H_2O in order to make a 4×10^{-5} M solution. Metal ($CuCl_2$) was dissolved in H_2O in order to prepare a 4×10^{-4} M solution. The [d(CpG) + Metal] solutions were mixed together prior to obtaining the mass spectra.

Computational Methods. *Ab initio* calculations were performed with 6-31G(d) basis sets to determine optimized structures and energies. Density functional theory (DFT) at the B3LYP level was carried out using the Gaussian09[32] series program. DFT was chosen because DFT is less computationally demanding than other computational methods with a similar accuracy in a ground-state energy calculation.[33] Vibrational frequencies were also calculated at the B3LYP level to confirm the optimized geometries corresponding to true minima on the potential energy surface.

Results and Discussion

MS and MS/MS spectra of the [Cu(I)·d(CpG)·d(CpG) – 2H]$^{-1}$ complex were used for the investigation of the Cu binding site without a DNA backbone. The gas-phase *m/z* 555 [d(CpG) – H]$^{-1}$, *m/z* 1111 [d(CpG)·d(CpG) – H]$^{-1}$, and *m/z* 1173 [Cu(I)·d(CpG)·d(CpG) – 2H]$^{-1}$ complexes were observed as stable complex ions in the various electrospray source-conditions. The low-energy CID MS/MS results of three complexes are summarized in Table 1.

ESI-MS and MS/MS Spectra of d(CpG) Solution. The ESI mass spectrum of the d(CpG) solution showed two peaks at *m/z* 555 and 1111 that corresponded to [d(CpG) – H]$^{-1}$ and [d(CpG)·d(CpG) – H]$^{-1}$, respectively, as shown in Figure 1(a). The [d(CpG) – H]$^{-1}$ peak intensity was the highest intensity because of the deprotonation of phosphate group in the d(CpG) molecule. In Figure 1(b) MS/MS spectrum, [d(CpG) – H – Cyt]$^{-1}$ and [d(CpG) – H – Cyt – dR]$^{-1}$ fragment ions were observed as the typical fragment ions of the parent [d(CpG) – H]$^{-1}$ ion. As a result of this MS/MS fragment ions, the weak bond of the [d(CpG) – H]$^{-1}$ ion was thought to be located at the N1(cytosine)-glycoside bond between cytosine base and deoxyribose (dR). In the MS/MS spectrum (Figure 1(c)), the [d(CpG) – H]$^{-1}$ fragment ion was observed as the main fragment ion of the parent [d(CpG)·d(CpG) – H]$^{-1}$ ion. The weak bond of the parent [d(CpG)·d(CpG) – H]$^{-1}$ duplex ion was thought to be located between two mononucleotides. The [d(CpG) – H – Cyt]$^{-1}$ (*m/z* 444) and [d(CpG) – H – Cyt – dR]$^{-1}$ (*m/z* 346) fragment ions were also observed with the low intensity peaks in Figure 1(c).

ESI-MS and MS/MS Spectra of (Cu + d(CpG)) Solution. The ESI mass spectrum of the (Cu + d(CpG)) solution showed two peaks at *m/z* 555 and 1173 that corresponded to [d(CpG) – H]$^{-1}$ and [Cu(I)·d(CpG)·d(CpG) – 2H]$^{-1}$, respectively, as shown in Figure 1(d). The [Cu(I)·d(CpG) – 2H]$^{-1}$ (*m/z* 617), [Cu(I)·d(CpG) – 2H – Cyt]$^{-1}$ (*m/z* 506), and [Cu(I)·d(CpG) – 2H – Cyt – dR]$^{-1}$ (*m/z* 408) fragment ions were observed as the typical fragment ions in the MS/MS spectrum of the parent [Cu(I)·d(CpG)·d(CpG) – 2H]$^{-1}$ ion (Figure 1(e)). No differences were observed in the MS/MS fragmentation patterns between two parent ions ([d(CpG)·d(CpG) – H]$^{-1}$ and [Cu(I)·d(CpG)·d(CpG) – 2H]$^{-1}$ ion). Three dissociation channels ((1) d(CpG) loss, (3) {d(CpG) +

Table 1. Fragment ions in the MS/MS spectra of Figure 1(b), 1(c) and 1(e)

Parent ion	Fragment ion (*m/z*)	Assignment	Dissociation channel
Figure 1(b), [d(CpG) – H]$^{-1}$ *m/z* 555	444	[d(CpG) – H – Cyt]$^{-1}$	
	346	[d(CpG) – H – Cyt – dR]$^{-1}$	
Figure 1(c), [d(CpG)·d(CpG) – H]$^{-1}$ *m/z* 1111	555	[d(CpG) – H]$^{-1}$	
	444	[d(CpG) – H – Cyt]$^{-1}$	
	346	[d(CpG) – H – Cyt – dR]$^{-1}$	
Figure 1(e), [Cu(I)·d(CpG)·d(CpG) –2H]$^{-1}$ *m/z* 1173	617	[Cu(I)·d(CpG) – 2H]$^{-1}$	(1)
	555	[d(CpG) – H]$^{-1}$	(2)
	506	[Cu(I)·d(CpG) – 2H – Cyt]$^{-1}$	(3)
	408	[Cu(I)·d(CpG) – 2H – Cyt – dR]$^{-1}$	(4)

Cyt} loss, and (4) {d(CpG) + Cyt +dR} loss channels) were observed as the common dissociation channels (Figure 1(c) and 1(e)). Because of the observation of two fragment ions (*m/z* 408 and m/ 506, dissociation channel (3) and (4)) in Figure 1(e), Cu cation is not thought to be bound at cytosine base area of the d(CpG)·d(CpG) molecule even though Cu cation could have a possibility to interact freely with N3 or N4 atom of cytosine base in the d(CpG)·d(CpG) molecule.

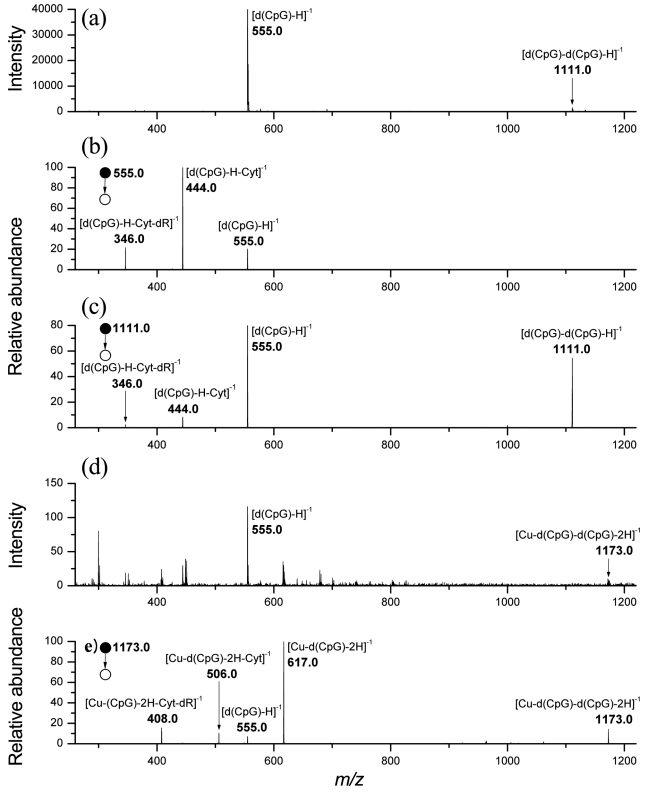

Figure 1. (a) ESI-MS spectrum of the d(CpG) solution in H_2O; (b) ESI-MS/MS spectrum of *m/z* 555 $[d(CpG) - H]^{-1}$ parent ion, and (c) of *m/z* 1111 $[d(CpG)\cdot d(CpG) - H]^{-1}$ parent ion; (d) ESI-MS spectrum of (Cu + d(CpG) solution in H_2O; (e) ESI-MS/MS spectrum of *m/z* 1173 $[Cu(I)\cdot d(CpG)\cdot d(CpG) - 2H]^{-1}$ parent ion.

Structure and Energy Analysis of $[Cu(I)\cdot d(CpG)\cdot d(CpG) - 2H]^{-1}$ Complex. From the five possible input geometries (Figure 2), the five output geometries of the $[Cu(I)\cdot d(CpG)\cdot d(CpG) - 2H]^{-1}$ complex were optimized. Three geometries ("a"–"c") for the Watson-Crick complex form and two geometries ("d" and "e") for the interstrand complex form are shown. Cu cation binds to the negatively charged phosphate group (Figure 2(a)), or the N7 of the guanine and phosphate group of same strand (Figure 2(b)), or O2 of the cytosine and N2 of the guanine (Figure 2(c)) which does not disrupt the C–G Watson-Crick triple hydrogen bonds. In the "b" geometry, it was necessary that the phosphate group and guanine base were not at the same nucleotide. In the interstrand complex form as shown in Figure 2(d), Cu cation chelates with the N7 and O6 of guanine on one strand and N3 and O2 of cytosine on the complementary strand. Further, as shown in Figure 2(e), Cu cation chelates with the O2 of cytosine and O6 of guanine on one strand and with O2 of cytosine and O6 of guanine on the complementary strand like a globular structure as reported by Baker *et al.*[20] The "d" geometry was optimized as the most energetically favorable structure at B3LYP/6-31G(d) level quantum chemistry calculations (Table 2). Relative energies and optimized geometric parameters are summarized in Table 2 and 3. Among the four-coordination structures, two square-planar geometries

Table 2. SCF energies of the five optimized $[Cu(I)\cdot d(CpG)\cdot d(CpG) - 2H]^{-1}$ complex ions in B3LYP/6-31G(d) calculations

	SCF Energy	
	B3LYP/6-31G(d) (hartree)	Δ^a (kcal/mol)
"a"	-6180.82127936	46.3
"b"	-6180.89510491	0.0
"c"	-6180.86176138	20.9
"d"	-6180.92229972	-17.1
"e"	-6180.90429726	-5.8

[a]Energy difference = Energy ("n") – Energy ("b")

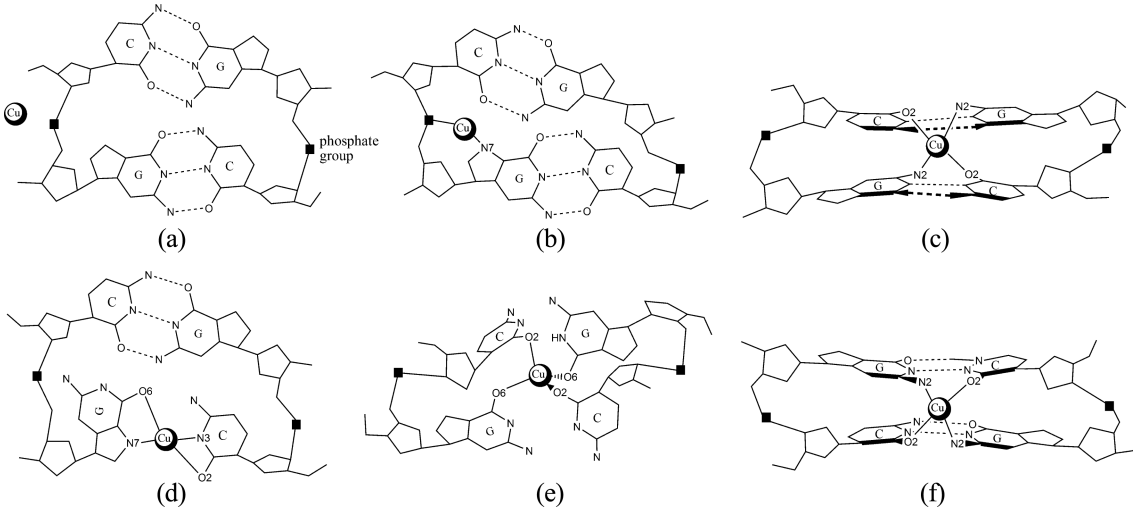

Figure 2. Five input geometries for $[Cu(I)\cdot d(CpG)\cdot d(CpG) - 2H]^{-1}$ complex ion. (a) "a" (b) "b" (c) "c" (front view) (d) "d" (e) "e" (f) "c" geometry (back view).

and a tetrahedral geometry were considered for the geometry optimization. The five atoms (Cu cation, O2, N2, O2, N2) of the "c" geometry are not located in the same plane (Figure 2(c)). While the five atoms(Cu cation, N7, O6, N3, O2) of the "d" geometry are located in the same plane (Figure 2(d)). In the four-coordination "e" geometry, the five atoms (Cu cation, O2, O6, O2, O6) were optimized to a tetrahedral structure as shown in Figure 2(e).

The "a" and "b" geometries were thought to be suitable for two dissociation channels (1 and 2, *m/z* 617 and *m/z* 555) that were observed in the MS/MS spectrum of the parent [Cu(I)·d(CpG)·d(CpG) – 2H]$^{-1}$ ion (Figure 1(e)). Between "a" and "b" geometries, "b" geometry was thought to be suitable for the [Cu(I)·d(CpG)·d(CpG) – 2H]$^{-1}$ complex because of –46.3 kcal/mol relative energy difference in the B3LYP/6-31G(d) calculations (Table 2). The [Cu(I)·d(CpG) – 2H–Cyt]$^{-1}$ (dissociation channel 3, *m/z* 506) and [Cu(I)·d(CpG) – 2H – Cyt – dR]$^{-1}$ (dissociation channel 4, *m/z* 408) fragment ions could be also considered to originate from the "b" geometry under our low-energy CID condition. As a result, the "b" geometry is regarded as a main complex geometry for the [Cu(I)·d(CpG)·d(CpG) – 2H]$^{-1}$ complex formation. It also seemed that the "c" geometry was not suitable for the observation of the [Cu(I)·d(CpG) – 2H]$^{-1}$ fragment ion (dissociation channel 1, *m/z* 617) in Figure 1(e). The bond breakages of two metal-ligand (Cu-O and Cu-N) and two triple hydrogen bonds are needed to observe the [Cu(I)·d(CpG) – 2H]$^{-1}$ fragment ions from the "c" geometry complex. However, two breakages of triple hydrogen bonds are enough to observe the [Cu(I)·d(CpG) – 2H]$^{-1}$ fragment ions

Table 3. Optimized geometric parameters of [Cu(I)·d(CpG)·d(CpG) – 2H]$^{-1}$ complex ions in B3LYP/6-31G(d) calculations

Geometry	Bond distance (Å)			
"a"	O1-Cu (1.966)	O2-Cu (1.967)		
"b"	O1-Cu (1.857)	O2-Cu (2.948)	N7(Gua1)-Cu (1.848)	
"c"	O2(Cyt1)-Cu (2.211)	N2(Gua1)-Cu (1.962)	O2(Cyt2)-Cu (2.215)	N2(Gua2)-Cu (1.963)
"d"	N7(Gua1)-Cu (1.825)	O6(Gua1)-Cu (3.151)	N3(Cyt2)-Cu (1.844)	O2(Cyt2)-Cu (2.804)
"e"	O2(Cyt1)-Cu (2.145)	O6(Gua1)-Cu (2.034)	O2(Cyt2)-Cu (2.054)	O6(Gua2)-Cu (1.957)
Geometry	Bond angle (°)			
"a"	O1-Cu-O2 (90.0)			
"b"	Cu-O1-O2 (80.2)	N7(Gua1)-Cu-O1 (159.6)		
"c"	O2(Cyt1)-Cu-N2(Gua1) (101.7)	N2(Gua1)-Cu-O2(Cyt2) (83.6)	O2(Cyt2)-Cu-N2(Gua2) (101.5)	N2(Gua2)-Cu-O2(Cyt1) (83.7)
"d"	Cu-N7(Gua1)-O6(Gua1) (74.1)	N7(Gua1)-Cu-N3(Cyt2) (167.5)	Cu-N3(Cyt2)-O2(Cyt2) (85.0)	
"e"	O2(Cyt1)-Cu-O6(Gua1) (96.6)	O6(Gua1)-Cu-O2(Cyt2) (108.9)	O2(Cyt2)-Cu-O6(Gua2) (123.4)	O6(Gua2)-Cu-O2(Cyt1) (112.5)
Geometry	Dihedral angle (°)			
"a"	O1-Cu-O2-P (-2.1)			
"b"	Cu-O1-P-O2 (-39.2)	N7(Gua1)-Cu-O1-O2 (-29.9)		
"c"	N2(Gua1)-O2(Cyt1)-N2(Gua2)-Cu (-9.3)	N2(Gua2)-O2(Cyt2)-N2(Gua1)-Cu (-9.3)	O2(Cyt1)-N2(Gua2)-O2(Cyt2)-Cu (28.9)	O2(Cyt1)-N2(Gua2)-O2(Cyt2)-N2(Gua1) (39.8)
"d"	O6(Gua1)-N7(Gua1)-O2(Cyt2)-Cu (3.9)	O2(Cyt2)-N3(Cyt2)-O6(Gua1)-Cu (-2.9)	O6(Gua1)-N7(Gua1)-O2(Cyt2)-N3(Cyt2) (-7.5)	
"e"	O2(Cyt1)-O6(Gua1)-O2(Cyt2)-Cu (-41.3)	O2(Cyt2)-O6(Gua2) O2(Cyt1)-Cu (-22.9)	O6(Gua1)-O2(Cyt2)-O6(Gua2)-Cu (38.4)	

from the "b" geometry complex.

The other two interstrand geometries ("d" and "e" geometries) have strong metal-ligand bonds between Cu cation and two bases in the $[Cu(I)\cdot d(CpG)\cdot d(CpG) - 2H]^{-1}$ complex. These two geometries were not suitable for the explanation of MS/MS spectrum as observed in Figure 1(e), even though the "d" geometry was calculated as the most stable geometry in B3LYP/6-31G(d) energy calculations (Table 2). If the $[Cu(I)\cdot d(CpG)\cdot d(CpG) - 2H]^{-1}$ complex had one of these two geometries, the {d(CpG) + Gua} loss and {d(CpG) + Cyt} loss fragment ions had to be observed as an equal probability because of the symmetric $[Cu(I)\cdot d(CpG)\cdot d(CpG) - 2H]^{-1}$ complex structure. However, the {d(CpG) + Gua} loss (or {d(CpG) + Gua + dR} loss) fragment ions were not observed in the MS/MS spectrum of the parent $[Cu(I)\cdot d(CpG)\cdot d(CpG) - 2H]^{-1}$ ion (Figure 1(e)). Therefore, these two interstrand geometries ("d" and "e") were not thought to be the principal complex forms in our experimental condition.

Conclusions

It has been demonstrated through ESI-MS analysis that guanine base (rather than cytosine base) was the preferred Cu cation binding site in a $[Cu(I)\cdot d(CpG)\cdot d(CpG) - 2H]^{-1}$ complex without a DNA backbone. No differences were observed in the MS/MS fragmentation patterns between two $[d(CpG)\cdot d(CpG) - H]^{-1}$ and $[Cu(I)\cdot d(CpG)\cdot d(CpG) - 2H]^{-1}$ parent ions, with the common observation of three fragment ions due to loss of d(CpG), {d(CpG) + Cyt}, and {d(CpG) + Cyt + dR}. Therefore, the Cu cation binding sites were proposed to be the N7 of the guanine and phosphate group of the same strand, as shown in the "b" geometry. This structure had the most stable geometry among the three Watson-Crick forms at B3LYP/6-31G(d) level energy calculations. Two optimized interstrand geometries of the $[Cu(I)\cdot d(CpG)\cdot d(CpG) - 2H]^{-1}$ complex ion were also reported.

Acknowledgments. This paper was supported by Research Fund, Kumoh National Institute of Technology.

References

1. Liu, H.-K.; Sadler, P. J. *Acc. Chem. Res*. **2011**, *44*, 349.
2. Yanga, H.; Meterab, K. L.; Sleimana, H. F. *Coord. Chem. Rev.* **2010**, *254*, 2403.
3. Clever, G. H.; Kaul, C.; Carell, T. *Angew. Chem. Int. Ed.* **2007**, *46*, 6226.
4. Eichhorn, G. L.; Clark, P. *Proc. Natl. Acad. Sci.* **1965**, *53*, 586.
5. Eichhorn, G. L. *Nature* **1962**, *194*, 474.
6. Berg, J. M.; Tymoczko, J. L.; Stryer, L. *Biochemistry*, 7th Ed., W. H. Freeman and Company, 2012.
7. Cambell, N. A. *Biology*, 4th Ed., Benjamin/Cummings Publishing Company, Inc., Menlo Park, CA, 1996.
8. Burrows, C. J.; Muller, J. G. *Chem. Rev.* **1998**, *98*, 1109.
9. Lippert, B. *Coord. Chem. Rev.* **2000**, *200*, 487.
10. Sigel, A.; Sigel, H. *Probing of Nucleic Acids by Metal Ion Complexes of Small Molecules*; Metal Ions in Biological Systems, Vol. 33; Dekker: New York, 1996.
11. Woisard, A.; Fazakerley, G. V.; Guschlbauer, W. *J. Biomol. Struct. Dynam.* **1985**, *2*, 1205.
12. Zimmer, C. H.; Luck, G.; Fritzsche, H.; Thiebel, H. *Biopolymers* **1971**, *10*, 441.
13. Hackl, E. V.; Kornilova, S. V.; Kapinos, L. E.; Andrushchenko, V. V.; Galkin, V. L.; Grigoriev, D. N.; Blagoi, Y. P. *J. Mol. Struct*. **1997**, *408*, 229.
14. Andrushchenko, V.; Van De Sande, J. H.; Wieser, H. *Biopolymers* **2003**, *72*, 374 .
15. Gao, Y.-G. ; Sriram, M.; Wang, A. H.-J. *Nucleic Acids Res.* **1993**, *21*, 4093.
16. B. Blažič, B.; Turel, I.; Bukovec, N.; Bukovec, P.; Lazarini, F. *J. Inorg. Biochem.* **1993**, *51*, 737.
17. Liu, J.; Lu, T. B.; Deng, H.; Ji, L. N.; Qu, L. H.; Zhou, H. *Transition Met. Chem*. **2003**, *28*, 116.
18. Atwell, S.; Meggers, E.; Spraggon, G.; Schultz, P. G. *J. Am. Chem. Soc*. **2001**, *123*, 12364.
19. Sissoëff, I.; Grisvard, J.; Guillé, E. *Prog. Biophys. Mol. Biol*. **1978**, *31*, 165.
20. Baker, E. S.; Manard, M. J.; Gidden, J.; Bowers, M. T. *J. Phys. Chem. B* **2005**, *109*, 4808.
21. Breslow, E.; Girotti, A. W. *J. Biol. Chem.* **1966,** *241*, 5651.
22. Cheng, P.; Bohme, D. K. *J. Phys. Chem. B* **2007**, *111*, 11075.
23. Fiskint, A. M.; Beer, M. *Biochem*. **1965**, *4*, 1289**.**
24. Xiang, Y.; Abliz, Z. *J. Am. Soc. Mass Spectrom*. **2004**, *15*, 689.
25. Sorokin, V. A.; Valeev, V. A.; Gladchenko, G. O.; Sysa, I. V.; Blagoi, Y. P.; Volchok, I. V. *J. lnorg. Biochem*. **1996**, *63*, 79.
26. Kim, M.-J.; Kim, B.-R.; Kim, H.-T. *Chem. Phys. Lett*. **2011**, *505*, 57.
27. Brancolini, G.; Felice, R. D. *J. Phys. Chem. B* **2008**, *112*, 14281.
28. Robertazzi, A.; Platts, J. A. *J. Biol. Inorg. Chem*. **2005**, *10*, 854.
29. Poater, J.; Sodupe, M.; Bertran, J.; Solà, M. *Mol. Phys.* **2005**, *103*, 163.
30. Noguera, M.; Bertran, J.; Sodupe, M. *J. Phys. Chem. A* **2004**, *108*, 333.
31. Aoki, K.; Clark, G. R.; Orbell, J. D. *Biochim. Biophys. Acta* **1976**, *425*, 369.
32. Gaussian 09, Revision A.1, Frisch, M. J.; Trucks, G. W.; Schlegel, H. B.; Scuseria, G. E.; Robb, M. A.; Cheeseman, J. R.; Scalmani, G.; Barone, V.; Mennucci, B.; Petersson, G. A.; Nakatsuji, H.; Caricato, M.; Li, X.; Hratchian, H. P.; Izmaylov, A. F.; Bloino, J.; Zheng, G.; Sonnenberg, J. L.; Hada, M.; Ehara, M.; Toyota, K.; Fukuda, R.; Hasegawa, J.; Ishida, M.; Nakajima, T.; Honda, Y.; Kitao, O.; Nakai, H.; Vreven, T.; Montgomery, J. A., Jr.; Peralta, J. E.; Ogliaro, F.; Bearpark, M.; Heyd, J. J.; Brothers, E.; Kudin, K. N.; Staroverov, V. N.; Kobayashi, R.; Normand, J.; Raghavachari, K.; Rendell, A.; Burant, J. C.; Iyengar, S. S.; Tomasi, J.; Cossi, M.; Rega, N.; Millam, J. M.; Klene, M.; Knox, J. E.; Cross, J. B.; Bakken, V.; Adamo, C.; Jaramillo, J.; Gomperts, R.; Stratmann, R. E.; Yazyev, O.; Austin, A. J.; Cammi, R.; Pomelli, C.; Ochterski, J. W.; Martin, R. L.; Morokuma, K.; Zakrzewski, V. G.; Voth, G. A.; Salvador, P.; Dannenberg, J. J.; Dapprich, S.; Daniels, A. D.; Farkas, Ö.; Foresman, J. B.; Ortiz, J. V.; Cioslowski, J.; Fox, D. J. Gaussian, Inc., Wallingford CT, 2009.
33. Sousa, S. F.; Fernandes, P. A.; Ramos, M. J. *J. Phys. Chem. A* **2007**, *111*, 10439.